International Journal of Sciences and Techniques of Automatic control & computer engineering
IJ-STA, Volume 4, N° 2, December 2010, pp. 1370-1387.

Maximum-Torque and Maximum-Efficiency Rotor Flux Selection of an Induction Motor in Transient Regime

Adnene Ben Ali [2,3], Riadh Abdelati [1,3], M. Faouzi Mimouni [1,3], R.Dhifaoui [2,3]

1. *National school of Engineers of Monastir, 5019 Monastir, Tunisia*;

2. INSA Tunis;

3. Research Unit "Network and Electrical Machines";

E-Mail: riaabdelati@yahoo.fr *E-Mail: Mfaouzi.mimouni@enim.rnu.tn*

Abstract: *A new control strategy for Induction Motor (IM) operating at variable speed and torque is proposed in this paper. In the high speed region, the measure of rotor speed and the sensitivity to IM's parameters of the motor still remains a problem. In this context, one proposes a neural approach that ensures sensorless control and maximum torque operation. The entire purpose is to introduce a new torque maximization approach by using optimal control theory. The optimal control provides dynamic regimes with a minimum input energy. This controller design is based on a d–q IM model and allows a decoupled control of the speed and flux. Taking into account dynamic equations of the speed and rotor flux with the voltage and current boundaries constraints, the flux reference is founded to achieve the maximum torque and minimum energy at any given speed. This optimal rotor flux is implemented in a Rotor Field Oriented Control (RFOC). Aiming to check it validity, this RFOC is implemented on a 1.5 kW laboratory IM. Comparing to a conventional control law, we have obtained better performances since lowest energy consumption and the highest torque are reached in an accelerated and motoring mode.*

Keywords: *Induction motor, optimal control, maximum torque, energy minimization, dynamic regime, neural network.*

I. Introduction

The conventional RFOC method operating at constant rotor flux norm fixed at its standard level provides high- performance motion when the system operates at its standard operating point. Far from this, the machine's efficiency decreases; it can

This paper was recommended for publication in revised form by the editor Staff.
Edition: CPU of Tunis, Tunisia, ISSN: 1737-7749

result from a torque magnitude change or in some applications a high speed is required. Thus other modes of flux operation are required in order to reach system with optimal performances.

Many industrial applications such as spindle, mixers, traction, and vehicle drive need a maximum output torque and power developed by the electric machine in high-speed range. Therefore, in order to get a good dynamic performance, most of them used RFOC drives with a flux reference as the extra degree of freedom that can optimize the system operation. However, those applications required in the same time minimum energy consumption and maximum possible torque in the whole operating range.

Keeping on this framework, many recent papers deal with the problem of torque optimisation in both of the steady state operation and the transient regime. In steady state operation the optimization problem is restricted to maximize the output torque but in the dynamic operation to optimize this variable means to maximize it when the motor is accelerated and to minimize in the deceleration mode. The torque is considered positive during motoring and negative for generating.

J. Soltani et al. [1] presented a maximum torque per ampere control strategy used the rotor flux as a control variable. For a given rotor speed and load torque a stator current is minimized in order to obtain an online optimized rotor flux. By the help of adaptive rotor flux and speed observer, an optimal direct flux field orientation control of induction motor is studied. Koichiro Nagata et al. [2] proposed a high-torque control in the low speed range with sensorless induction motor drive. The proposed method is based on the control of the slip angular frequency and it's subjected to the problems of both higher starting torque and impact load. A Banbury mixer is given as an example of a higher start torque demand. Only steady state operation is considered in this study. H. Abu-Rub et al. [3] presented a maximum-torque approach based on field weakening technique and by taking into account both the maximum inverter voltage and current. Three regions are defined by the physical limits of the inverter's voltage and currents. The control algorithm is implemented as a sensorless scheme in a rotor flux oriented system. Copper and iron losses minimization approach and maximum torque per ampere control were studied in [4]. The authors proposed a scalar control scheme implemented in a constant V/f control. In order to reduce the number of the PI regulators in the field-oriented control, authors in [5] used the stator flux components as control variables instead of the stator currents components. Their proposed method allows the induction motor to exploit the maximum torque by decreasing the direct stator flux component as soon as the request voltage tends to overcome the available. S. Lim and K. Nam [6] proposed both minimization of the loss in the motor and maximum torque strategy based on the Kuhn-Tucker theorem. Three physical limit-regions are defined for the maximum torque. An optimal flux reference is generated from an online optimal flux command algorithm implemented in the rotor flux oriented control. Jul-Ki Seok et al. [7] proposed a maximum torque operation approach that maintains some robustness to parameter error in the flux-weakening region. In [8], the authors presented a maximum or minimum torque method subject to the inverter' voltage and current capability and occurred in both the motor and the generator modes and it defined in three regions. For each region a torque optimization is determined from motoring mode and a second one for the generating mode. These maximum and minimum torques are obtained from analytical

resolutions. Their approach is implemented and compared to a standard field-weakening method.
In this paper, an original technique leading to determine the optimal rotor flux in dynamic regime that allows to the motor an optimal torque. A positive torque and an accelerate mode of the motor speed are chosen. This torque-optimizing strategy is inspired from theories studies dealing with optimal control problem focus on the optimizing energy of AC motors and subjected to the inverter' voltage and current capability limit. In the other word, the proposed strategy is consisting of minimizing a cost function given as an integral of a weighted sum of energetic model of the IM and by taking into account the boundary conditions on stator voltages and currents limits. The task is to find the optimal rotor flux that corresponds to the maximum torque value and provides the lowest IM's energy consumption along a given accelerate-motoring operation.
By means of numerical algorithm, both the optimizing rotor flux trajectory and the computed maximum torque are determined from a specific optimal control problem based on Kuhn-Tecker theorem [6]. By the help of the least square method an approximate time-varying optimal flux reference is implemented in the RFOC scheme. The given control law is the Optimal Rotor Field Oriented Control (ORFOC), gives both maximum induction motor efficiency and maximum torque for any given accelerated-motor speed range.
Because the measure of rotor speed In the high speed region and the sensitivity to parameters errors of the motor remains a problem, a neural algorithm of rotor speed estimation is developed in this paper.
This paper is organized as follows: the second section is devoted to describe the complete dynamic model of IM used in this work and the energetic model. In section three, we present the energy-loss cost function. In the fourth section, an optimal control strategy is presented in which, a maximum torque approach with minimum-energy consumption is developed based on the Kuhn-Tucker theorem. The resolution of the maximum torque strategy is developed in the fifth section. In the sixth section the optimal solutions are presented. The ORFOC used the proposed optimal rotor flux is presented in seventh section. In the eighth section, simulation results of the proposed strategy are compared to those given by an RFOC based on the standard field-weakening approach

2. Model of IM

2.1 Dynamic model of IM

The full-order dynamic model of an IM viewed from the synchronous rotating reference frame is given by (1) to (3) [9, page 501]:

$$\begin{cases} \dot{I}_s^{(d,q)} = -\left(\gamma I + \left(\omega_{slip} + p\Omega\right)J\right)I_s^{(d,q)} + \eta\left(aI - p\Omega J\right)\Phi_r^{(d,q)} + \dfrac{V_s^{(d,q)}}{\sigma L_s} & (1) \\ \dot{\Phi}_r^{(d,q)} = -\left(aI + \omega_{slip} J\right)\Phi_r^{(d,q)} + bI_s^{(d,q)} & (2) \\ \dot{\Omega} = -\dfrac{\tau_l}{J_m} + \dfrac{y}{J_m} & (3) \end{cases}$$

Where $I_s^{(d,q)} = \begin{bmatrix} I_{sd} \\ I_{sq} \end{bmatrix}$, $\Phi_r^{(d,q)} = \begin{bmatrix} \Phi_{rd} \\ \Phi_{rq} \end{bmatrix}$, $V_s^{(d,q)} = \begin{bmatrix} V_{sd} \\ V_{sq} \end{bmatrix}$ $I = \begin{bmatrix} 1 & 0 \\ 0 & 1 \end{bmatrix}$ and $J = \begin{bmatrix} 0 & -1 \\ 1 & 0 \end{bmatrix}$,

when *I*: is the 2x2 unit matrix and *J*: is the 2X2 skew symmetric matrix.

with ω_{slip}: as the sleep frequency, $\omega_r = p\Omega$: as the electrical rotor speed; I_{sd}, I_{sq}: as the magnetizing and torque currents respectively; $\dot{I}_{sd} = \dfrac{d}{dt} I_{sd}$, $\dot{I}_{sq} = \dfrac{d}{dt} I_{sq}$: are the differential of magnetizing and torque currents respectively; V_{sd}, V_{sq}: the stator voltage in d-q axis; Φ_{rd}, Φ_{rq}: rotor fluxes in d-q axis, p: pairs poles number; Ω: as the motor speed; τ_l: load torque; y: as the electromagnetic torque; J_m: is the total moment of inertia of the rotor and fly-wheel masses reduced to the motor shaft,

And $\gamma = \dfrac{1}{\sigma L_s}\left(R_s + \dfrac{M^2}{L_r^2} R_r\right)$, $\eta = \dfrac{M}{\sigma L_s L_r}$, $a = \dfrac{R_r}{L_r}$, $b = aM$, $\sigma = 1 - \dfrac{M^2}{L_s L_r}$

, with R_r and R_s are the rotor and stator resistances, L_r and L_s : The rotor and the stator inductance respectively and *M* is the magnetizing inductance.

As the case of many industrial applications, the load torque can be chosen as a function of the motor speed. In this paper, the load torque is chosen proportional to the motor speed. Then, the mechanical equation given in (3) can be expressed as follows:

$$\dot{\Omega} = -\frac{K_l}{J_m}\Omega + \frac{y}{J_m} \qquad (4)$$

With K_l: is the load torque constant.

The electromagnetic torque and the sleep frequency are given by the equations (5) and (6):

$$y = k\Phi_r I_{sq} \qquad (5)$$

$$\omega_{slip} = \frac{M}{T_r}\frac{I_{qs}}{\Phi_r} \qquad (6)$$

Where $k = \dfrac{3}{2}\dfrac{M}{L_r}$.

Finally, in the case of a decoupled control of the speed and the rotor flux as the case of RFOC: $\Phi_r^{(d,q)} = \begin{bmatrix} \Phi_r \\ 0 \end{bmatrix}$, the final IM model used in this paper is given as follows:

$$\begin{cases} \dot{I}_{sd} = -\gamma I_{sd} + \left(\dfrac{M}{T_r} \dfrac{I_{qs}}{\Phi_r} + p\Omega \right) I_{sq} + a\eta \Phi_r + \dfrac{V_{sd}}{\sigma L_s} & (7) \\ \dot{I}_{sq} = -\gamma I_{sq} - \left(\dfrac{M}{T_r} \dfrac{I_{qs}}{\Phi_r} + p\Omega \right) I_{sd} - \eta p \Omega \Phi_r + \dfrac{V_{sq}}{\sigma L_s} & (8) \\ \dot{\Phi}_r = -a\Phi_r + bI_{sd} & (9) \\ \dot{\Omega} = -\dfrac{K_l}{J_m}\Omega + \dfrac{k}{J_m}\Phi_r I_{sq} & (10) \end{cases}$$

2.2. Energy model of the induction motor

The input active power of an IM in rotating *dq*-frames is given by:

$$P_a = \frac{3}{2}\left(V_s^{(d,q)}\right)^T I_s^{(d,q)} \quad (11)$$

From equation (1), the input power is given by:

$$P_a = \frac{3}{2}\sigma L_s \left(\left(\dot{I}_s^{(d,q)} \right)^T \left(I_s^{(d,q)} \right) + \gamma \left(I_s^{(d,q)} \right)^T \left(I_s^{(d,q)} \right) - \eta a \left(\Phi_r^{(d,q)} \right)^T I_s^{(d,q)} \right) + \frac{3}{2}\sigma L_s \left(+ \eta p \Omega \left(\Phi_r^{(d,q)} \right)^T J I_s^{(d,q)} \right) \quad (12)$$

The relation between the stator and rotor currents can be given as follows:

$$I_s^{(d,q)} = \frac{1}{M}\left(\Phi_r^{(d,q)} - L_r I_r^{(d,q)} \right) \quad (13)$$

The instantaneous active power is then given by:

$$P_a = \frac{3}{2}\sigma L_s \left(\dot{I}_s^{(d,q)} \right)^T I_s^{(d,q)} + \frac{1}{L_r} \left(\dot{\Phi}_r^{(d,q)} \right)^T \Phi_r^{(d,q)} + R_s \left(I_s^{(d,q)} \right)^T I_s^{(d,q)} + \frac{3}{2}\left(+ R_r \left(I_r^{(d,q)} \right)^T I_r^{(d,q)} \right) + \Omega y \quad (14)$$

Finally we obtain the following active power expression:

$$P_a = \frac{d}{dt} W + P_J + P_m \quad (15)$$

Where

$$W = \frac{3}{2}\left(\frac{\sigma L_s}{2} \left(I_s^{(d,q)}\right)^T I_s^{(d,q)} + \frac{1}{2L_r} \left(\Phi_r^{(d,q)}\right)^T \Phi_r^{(d,q)} \right) \tag{16}$$

is the stored magnetic energy of the induction machine and the total copper losses can be written as:

$$P_J = \frac{3}{2}\left(\left(R_s + R_r \left(\frac{M}{L_r}\right)^2 \right) \left(I_s^{(d,q)}\right)^T I_s^{(d,q)} - \frac{R_r}{L_r^2} \left(\Phi_r^{(d,q)}\right)^T \Phi_r^{(d,q)} - \frac{2}{L_r} \left(\Phi_r^{(d,q)}\right)^T \left(\dot{\Phi}_r^{(d,q)} \right) \right) \tag{17}$$

The mechanical power transmitted to the IM rotor can be expressed as:

$$P_m = \Omega y \tag{18}$$

At the high speed range, the iron losses have a significant effect. But they do not figure in the Park model of the induction machine, unless they can be expressed as a function of the synchronous speed ω_s and the air gap flux Φ_m as given in the equation (19). At the same time, taking in the account these kinds of losses, make the eventual optimal control difficult to resolve. In order to simplify the algorithm, we can assign to the iron losses its maximum value (at $\Omega = \Omega_{\max}$).

From many former works, the iron losses can be expressed as follows [6], [9] and [10]:

$$P_f = \frac{3}{2}\left(K_h \left|\omega_s\right| + K_e \omega_s^2\right) \Phi_m^T \Phi_m \tag{19}$$

with K_h , K_e: as the eddy and hysteresis currents coefficient. The equation (19) can be simplified according to the small value of slip: s, the air gap flux can be expressed as $\Phi_m^T \Phi_m = \left(\frac{M}{L_r}\right)^2 \Phi_r^T \Phi_r$, and the electromagnetic torque is written as:

$$y = \frac{c}{b} \left\| \Phi_r^{(a,b)} \right\|^2 \dot{\rho} \tag{20}$$

where *c*: is the factor dependent on the way of transforming three-phase IM variables into two-phase ones . The synchronous speed can be derived as

$$\omega_s = p\Omega + \frac{by}{c\Phi_r^2} \tag{21}$$

The iron losses, in equation (19) can be rewritten as:

$$P_f = \frac{3}{2}\frac{M^2}{L_r^2}\left(K_h \left(\frac{b}{c}\frac{y}{\left\|\Phi_r\right\|^2} + p\Omega \right) + K_e \left(\frac{b}{c}\frac{y}{\left\|\Phi_r\right\|^2} + p\Omega \right)^2 \right) \Phi_r^T \Phi_r \tag{22}$$

This expression can be delimited as follows:

$$P_f < \frac{3}{2}\frac{M^2}{L_r^2}\left(K_h \left(\frac{b}{c} y + p\Omega_{\max} \left\|\Phi_r\right\|^2 \right) + K_e \left(\frac{b}{c}\frac{y}{\left\|\Phi_r\right\|} + p\Omega_{\max} \left\|\Phi_r\right\| \right)^2 \right) \tag{23}$$

This yield:

$$P_f < q_{f0}\Phi_r^T\Phi_r + r_{f0}\frac{y^2}{c\|\Phi_r\|^2} + k_f y \tag{24}$$

With $q_{f0} = \frac{3M^2}{2L_r^2}\left(K_h p\Omega_{\max} + K_e p^2\Omega_{\max}^2\right)$, $r_{f0} = \frac{3M^2}{2L_r^2}K_e b^2$, $k_f = \frac{b}{c}\left(K_h + 2K_e\Omega_{\max}\right)$

The third terms in (18) is independent of rotor flux and has no effect in the optimized problem. Given by the equation (19), the electromagnetic torque can be expressed as follows:

$$y = J\dot{\Omega} + K_l\Omega \tag{25}$$

Finally, a maximum value is predetermined for the iron losses and used in the minimum-energy algorithm. It can be given by the following expression:

$$P_f < \{P_f\}_{\Omega_{\max}} = q_{f0}\Phi_r^T\Phi_r + r_{f0}\frac{y^2}{c\|\Phi_r\|^2} \tag{26}$$

The term $k_f\left(J\dot{\Omega}_{\max} + K_l\Omega_{\max}\right)$ has no effect on the minimum-energy rotor flux trajectory, as consequence $\{P_f\}_{\Omega_{\max}}$ is chosen as given in (26).

3. Energy-loss cost function

An optimal control problem is based on minimizing a cost function. The cost function can be given as the integral of an index $f(I_{sd}, I_{sq}, \Phi_r, \Omega)$, given as follows:

$$J_r = \int_0^T f(I_{sd}, I_{sq}, \Phi_r, \Omega)dt \tag{27}$$

The index corresponds to the weighted sum of energy and losses:

$$f(I_{sd}, I_{sq}, \Phi_r, \Omega) = \alpha_1 W_L + \alpha_2 P_J + \alpha_3\{P_f\}_{\max} + \alpha_4 P_m \tag{28}$$

The weighting factors $\alpha_{i=1to4}$ are used to scale the combined power-energy of the criterion terms defined above. Minimizing the cost function consists on minimizing the magnetic energy W_L which corresponds to maximize the power factor and minimizing losses that increase the machine efficiency.
By using (16), (17), (18) and (26), and by taking into account the oriented rotor flux, the cost function is given as follows:

$$J_r = \frac{3\alpha_2}{2L_r}\left(\Phi_r^2(0)-\Phi_r^2(T)\right)+\frac{3}{2}\int_0^T\left(\alpha_1\left(\frac{\sigma L_s}{2}\left(I_{sd}^2+I_{sq}^2\right)+\frac{1}{2L_r}\Phi_r^2\right)\right)dt$$
$$+\frac{3}{2}\int_0^T\left(\alpha_2\left(R_s+R_r\left(\frac{M}{L_r}\right)^2\right)\left(I_{sd}^2+I_{sq}^2\right)+\frac{R_r}{L_r^2}\Phi_r^2-\frac{1}{L_r}\frac{d}{dt}\left(\Phi_r^2\right)\right)dt$$
$$+\frac{3}{2}\int_0^T\left(\frac{2}{3}\alpha_3\left(q_{f0}\Phi_r^2+r_{f0}\frac{y^2}{c\|\Phi_r\|^2}\right)+\frac{3}{2}\alpha_4 R_r\left(\frac{M}{L_r}\right)^2 I_{sq}^2+\frac{3}{2}\alpha_4\left(p\frac{M}{L_r}\right)\Phi_r I_{sq}\Omega)\right)dt \quad (29)$$

Rescaling the expression in (29), the cost function is given by the following expression:

$$J_r = K(\Phi_r(T))+\int_O^T\left(r_1 I_{sd}^2+r_2 I_{sq}^2+q_1\Phi_r^2+q_2\Phi_r I_{sq}\Omega\right)dt \quad (30)$$

with $K(\Phi_r(T))=\frac{3\alpha_2}{2L_r}\left(\Phi_r^2(0)-\Phi_r^2(T)\right)$ as the final state penalty term.

The weighting factors r_1, r_2, q_1 and q_2 are nonnegative constants, where:

$$r_1=\frac{3}{4}\sigma L_s\alpha_1+\frac{3}{2}(R_s+R_r\left(\frac{M}{L_r}\right)^2)\alpha_2,\quad r_2=r_1+r_{f0}\alpha_3+\frac{3}{2}\alpha_4 R_r\left(\frac{M}{L_r}\right)^2,$$
$$q_1=\frac{3}{4}\frac{\alpha_1}{L_r}-\frac{3}{2}\frac{R_r}{L_r^2}\alpha_2+q_{f0},\quad q_2=\frac{3}{2}p\frac{M}{L_r}\alpha_4$$

α_i are chosen on the way that q_1 is still positive.

4. Maximum torque approach with minimum-energy consumption

As given in section 3, a cost function was established in order to maximize the IM efficiency. Moreover, when this cost function is subjected to the stator voltages and currents boundaries, a positive maximum torque can be achieved accordingly. These boundary-conditions bring out three areas in which the motor is at either the current constraint, the voltage constraint or at both simultaneously.
The voltage constraint is given as follows:

$$V_{sd}^2+V_{sq}^2<V_{\max}^2 \quad (31)$$

where $V_{\max}=\frac{V_{DC}}{\sqrt{3}}$ and V_{DC} is the DC link voltage of the inverter.

And the current constraint is given by:

$$I_{sd}^2+I_{sq}^2<I_{\max}^2 \quad (32)$$

Where $I_{\max}$ is determined by the rating of the inverter's semiconductor switches.
The maximum-torque approach is presented as follows:
Find an optimal rotor flux trajectory $\Phi_r^*(t)$ that minimizes the cost function given in (30) and produces a maximum torque under the voltage and current constraints given in (31) and (32).

In order to maximize the motor torque, leads us to define three areas in the (I_{sd} , I_{sq}) space given by [6]:

$$\begin{cases} Area\_01 = \left\{ (I_{sd}, I_{sq}) / I_{sd}^2 + I_{sq}^2 < I_{\max}^2 \right\} \\ Area\_02 = \left\{ (I_{sd}, I_{sq}) / (I_{sd}^2 + I_{sq}^2 < I_{\max}^2) \cup (V_{sd}^2 + V_{sq}^2 < V_{\max}^2) \right\} \\ Area\_03 = \left\{ (I_{sd}, I_{sq}) / V_{sd}^2 + V_{sq}^2 < V_{\max}^2 \right\} \end{cases} \quad (33)$$

In other word, by the help of the Kuhn-Tucker theorem [6], the problem will be presented as follows:

Firstly, the Hamilton-Jacobi equation (HJE) [11] derived from the cost function J_r presented in (30) and the constraints presented in (31) and (32) is given as follows:

$$H = \left(r_1 I_{sd}^2 + r_2 I_{sq}^2 + q_1 \Phi_r^2 + q_2 \Phi_r I_{sq} \Omega \right) + \mu_1 (I_{sd}^2 + I_{sq}^2 - I_{\max}^2) + \mu_2 (V_{sd}^2 + V_{sq}^2 - V_{\max}^2) \quad (34)$$

with μ_1 and μ_2 are the Lagrange multipliers, chosen nonnegative constants.
In order to minimize the HJE, leads the following equations:

$$\frac{\partial H}{\partial I_{ds}} = 2 r_1 I_{ds} + 2 q_1 \Phi_r \frac{\partial \Phi_r}{\partial I_{ds}} + q_2 I_{qs} \left(\Omega \frac{\partial \Phi_r}{\partial I_{ds}} + \Phi_r \frac{\partial \Omega}{\partial I_{ds}} \right) + 2 \mu_1 I_{ds} + 2 \mu_2 \left(v_{qs} \frac{\partial v_{qs}}{\partial I_{ds}} + v_{ds} \frac{\partial v_{ds}}{\partial I_{ds}} \right) = 0 \quad (35)$$

$$\frac{\partial H}{\partial I_{qs}} = 2 r_2 I_{qs} + q_2 \Phi_r \Omega + q_2 I_{qs} \frac{\partial \Omega}{\partial I_{qs}} \Phi_r + 2 \mu_1 I_{qs} + 2 \mu_2 \left(v_{qs} \frac{\partial v_{qs}}{\partial I_{qs}} + v_{ds} \frac{\partial v_{ds}}{\partial I_{qs}} \right) = 0 \quad (36)$$

$$\mu_1 \left(I_{ds}^2 + I_{qs}^2 - I_{\max}^2 \right) = 0 \quad (37)$$

$$\mu_2 \left(v_{ds}^2 + v_{qs}^2 - v_{\max}^2 \right) = 0 \quad (38)$$

The conditions in (37) and (38) pilot the location of solution curves in such three areas presented in the system (33).

Therefore, in order to make easy the resolution of the equations (35)-(38), some simplifications are needed on the stator voltage expressions that can be derived from the equations (7) and (8). By taking into account the high-speed operation and by neglecting the stator resistance voltage drop and for small dynamics of the stator currents, the expressions of stator voltages are given from (7) and (8) as follows:

$$v_{ds} \approx -\left(\frac{M}{T_r}\frac{I_{qs}}{\Phi_r} + p\Omega\right)\sigma L_s I_{qs} \tag{39}$$

$$v_{qs} \approx \left(\frac{M}{T_r}\frac{I_{qs}}{\Phi_r} + p\Omega\right)\left(\frac{M}{L_r}\Phi_r + \sigma L_s I_{ds}\right) \tag{40}$$

Using (39) and (40), the expression in (38) becomes:

$$\mu_2\left(\left(\sigma^2 L_s^2 I_{ds}^2 + \sigma^2 L_s^2 I_{qs}^2 + \frac{M^2}{L_r^2}\Phi_r^2 + 2\frac{M}{L_r}\sigma L_s \Phi_r I_{ds}\right)\left(\frac{M^2}{T_r^2}\frac{I_{qs}^2}{\Phi_r^2} + p^2\Omega^2 + 2\frac{M}{T_r}\frac{I_{qs}}{\Phi_r}p\Omega\right) - v_{\max}^2\right) = 0 \tag{41}$$

Using the equations (7) and (9), the following terms can be expressed as follows:

$$\frac{\partial \Phi_r}{\partial I_{ds}} = \frac{\partial \Phi_r}{\partial t}\frac{\partial t}{\partial I_{ds}} = \left(-\frac{1}{T_r}\Phi_r + \frac{M}{T_r}I_{ds}\right)\frac{1}{-\gamma I_{ds} + I_{qs}\left(\frac{M}{T_r}\frac{I_{qs}}{\Phi_r} + p\Omega\right) + a\eta\Phi_r + \frac{v_{ds}}{\sigma L_s}} \tag{42}$$

The same development using (7), (8) and (10) yields:

$$\frac{\partial \Omega}{\partial I_{qs}} = \frac{-\frac{K_l}{J_m}\Omega + \frac{k}{J_m}\Phi_r I_{qs}}{-\gamma I_{qs} - I_{ds}\left(\frac{M}{T_r}\frac{I_{qs}}{\Phi_r} + p\Omega\right) - \eta p\Omega\Phi_r + \frac{v_{qs}}{\sigma L_s}} \tag{43}$$

$$\frac{\partial \Omega}{\partial I_{ds}} = \frac{-\frac{K_l}{J_m}\Omega + \frac{k}{J_m}\Phi_r I_{qs}}{-\gamma I_{ds} + I_{qs}\left(\frac{M}{T_r}\frac{I_{qs}}{\Phi_r} + p\Omega\right) + a\eta\Phi_r + \frac{v_{ds}}{\sigma L_s}} \tag{44}$$

Using (39) and (40), the partial derived expressions of stator voltage versus stator currents are given by the following equations:

$$\frac{\partial v_{ds}}{\partial I_{ds}} = \left(\frac{M}{T_r} \frac{I_{qs}}{\Phi_r^2} \left(\frac{\partial \Phi_r}{\partial I_{ds}} \right) - p \left(\frac{\partial \Omega}{\partial I_{ds}} \right) \right) \sigma L_s I_{qs} \tag{45}$$

$$\frac{\partial v_{ds}}{\partial I_{qs}} = -\left(\frac{2M}{T_r} \frac{I_{qs}}{\Phi_r} + p \left(\Omega + \left(\frac{\partial \Omega}{\partial I_{qs}} \right) I_{qs} \right) \right) \sigma L_s \tag{46}$$

$$\begin{aligned} \frac{\partial v_{qs}}{\partial I_{ds}} = & \left[\frac{M}{T_r} \left(1 - \frac{I_{ds}}{\Phi_r} \left(\frac{\partial \Phi_r}{\partial I_{ds}} \right) \right) \frac{I_{qs}}{\Phi_r} + p \left(\left(\frac{\partial \Omega}{\partial I_{ds}} \right) I_{ds} + \Omega \right) \right] \sigma L_s \\ & + p \frac{M}{L_r} \left(\Phi_r \left(\frac{\partial \Omega}{\partial I_{ds}} \right) + \Omega \left(\frac{\partial \Phi_r}{\partial I_{ds}} \right) \right) \end{aligned} \tag{47}$$

$$\frac{\partial v_{qs}}{\partial I_{qs}} = \left(\frac{M}{T_r} \frac{1}{\Phi_r} + p \left(\frac{\partial \Omega}{\partial I_{qs}} \right) \right) \left(\frac{M}{L_r} \Phi_r + \sigma L_s I_{ds} \right) \tag{48}$$

Moreover, in order to take into account both dynamic of motor speed and rotor flux, two joined constrained are needed in this Kuhn-Tucker resolution given as follows:

1- A transient motor speed defined by the following expression:

$$\Omega(t) = c_0 t + c_1 \begin{cases} 0 < \Omega < \Omega_{rated} & for\ Area\_01 \quad (49) \\ \Omega_{rated} < \Omega < 2\Omega_{rated} & for\ Area\_02 \quad (50) \\ 2\Omega_{rated} < \Omega < 3\Omega_{rated} & for\ Area\_03 \quad (51) \end{cases}$$

c_0 is chosen positive constant in order to obtain a motor's accelerated modes.

2- By taking into account the expression of the dynamic equation of the rotor flux given in (9), and in order to use a sample resolving algorithm, no closed-loop flux control is needed but only a sample step response of the rotor flux that can be calculated from this first-order differential (9) as far as the direct current is assumed to track its reference instantaneously, the rotor flux can be given by the following expression [7]:

$$\Phi_r((k+1)T_e) = MI_{ds}((k+1)T_e) + \left(\Phi_r(kT_e) - M\ I_{ds}(kT_e) \right) e^{-\left(\frac{kT_e}{T_r} \right)} \tag{52}$$

with T_e is the settling time and T_r is the rotor constant time.

Analytical resolution of the problem is difficult to obtain. But numerical resolution can be developed in order to obtain the minimum-energy rotor flux and maximum torque. That's why, the dynamic of the rotor flux given in (52) is given in numerical form.

Furthermore, by choosing a settling time T_e all the equations in above have been converted in numerical form.

5. Maximum torque approach resolution

Finally, by replacing the expressions (39)-(48) in both (35) and (36) and taking into account the equations (37), (41), (49), (50), (51) and (52) the problem is broken down into three numerical sub-algorithms:

i) **First Algorithm**:

($\mu_1 \neq 0$ and $\mu_2 = 0$) resolution of equations (35), (36) and (37).

The algorithm is given as follows: Every *k* step of the algorithm, solve the numerical form of the equation (35) and pick out the expression of $\mu^*_{1\_1}(k)$ versus $I^*_{ds\_1}(k)$, and $I^*_{qs\_1}(k)$, then solve the numerical form of the equation (37) to obtain the expression of $I^*_{ds\_1}(k)$ versus $I^*_{qs\_1}(k)$. From the numerical form of the equation (36) pick out the real values of $I^*_{qs\_1}(k)$ and then the unique value that satisfies the boundary limit. Store the values of the solutions $\left\{I^*_{ds\_1}(k), I^*_{qs\_1}(k) \textit{ and } \mu^*_{1\_1}(k)\right\}$, and using the equation (34) to store the HJE value of $H(k)$. Finally Minimum-energy rotor flux $\Phi^*_{r\_1}(k)$ and maximum torque $T^*_{e\_1}(k)$ trajectories in the area_1 can be derived from these solutions.

ii) **Second Algorithm**:

($\mu_1 \neq 0$ and $\mu_2 \neq 0$) resolution of equations (35), (36), (37) and (41).

As the algorithm explained in the area_01, the same principle is considered in area_02 to obtain the following solutions: $\left\{I^*_{ds\_2}(k), I^*_{qs\_2}(k), \mu^*_{1\_2}(k) \textit{ and } \mu^*_{2\_2}(k)\right\}$, and minimum-energy rotor flux $\Phi^*_{r\_2}(k)$ and maximum torque $T^*_{e\_2}(k)$ trajectories in the area_2 are then given.

iii) **Third Algorithm**:

($\mu_1 = 0$ and $\mu_2 \neq 0$) resolution of equations (35), (36) and (41).

Solutions are $\left\{I^*_{ds\_3}(k), I^*_{qs\_3}(k) \textit{ and } \mu^*_{2\_3}(k)\right\}$, using the equation (34) to confirm the minimum values of the HJE, minimum-energy rotor flux $\Phi^*_{r\_3}(k)$ and maximum torque $T^*_{e\_3}(k)$ trajectories in the area_3 can be derived from the above solutions.

6. Rotor speed Estimation using the neural approach

An Artificial neural network is characterized by its architecture, training or learning algorithms and activation functions. The architecture describes the connections between the neurons. It consists of an input layer, an output layer and generally, one or more hidden layers in-between. Fig. 1 illustrates one of the commonly used networks, namely, the layered feed-forward neural network with one hidden layer.

The layers in these networks are interconnected by communication links that are associated with weights that dictate the effect on the information passing through them. These weights are determined by the learning algorithm.

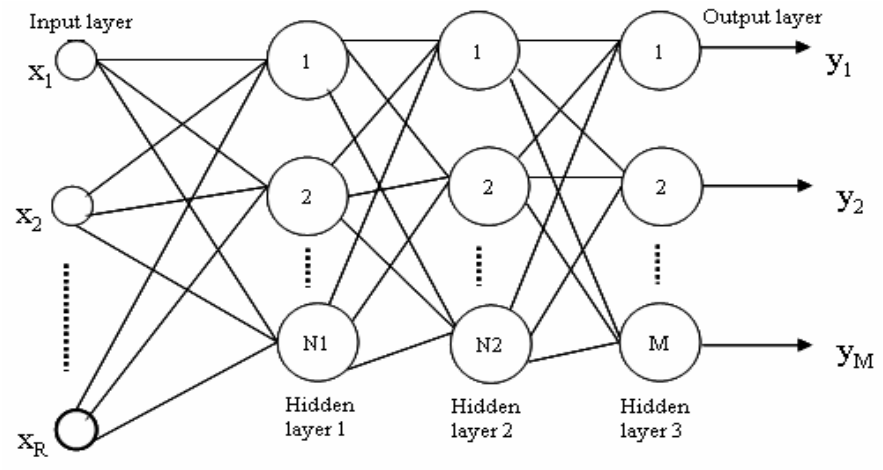

Figure(1): structure of neuronal networks

In this work and for this type of application, the neural network constitutes one hidden layer with a hyperbolic tangent activation function and output layer with linear function. The learning algorithm is the back-propagation algorithm.
The inputs of the neural network are the voltage and current. The output of the neural network model consists of one neuron representing the rotor speed.

Extensive simulations results are presented to evaluate the neural network estimation of the rotor speed.
We note in Fig. (2) the estimated rotor speed which converge to the real rotor speed in either low and high speed range.

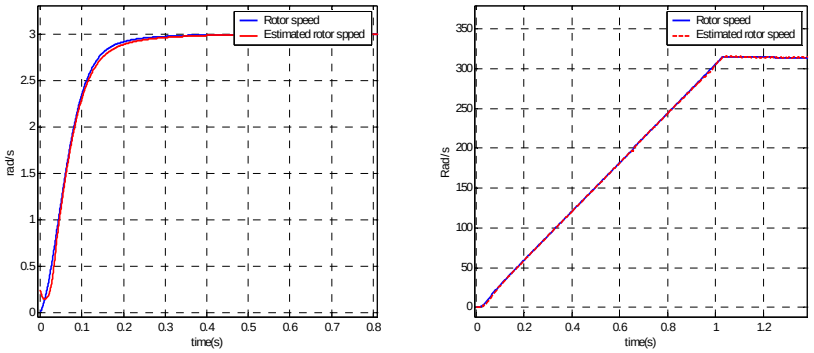

Figure (2) :simulation result of neural network estimation rotor speed

7. Optimum solutions results

7.1 First area

As given in (49), the area corresponds to an acceleration mode of the IM when the motor speed increase from 0rd/s to 147rd/s as illustrated in Figure (3) (the rated motor speed of our laboratory 1.5KW induction motor is 147 rd/s). Both of the maximum torque $T_{e\_1}^{*}(k)$ and the optimal rotor flux $\Phi_{r\_1}^{*}(k)$ are given respectively in figures (4) and (5).

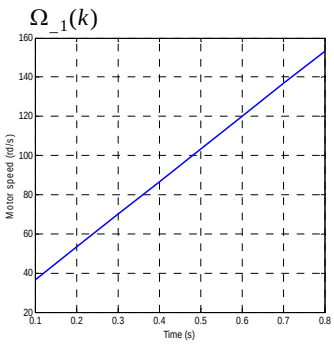

Figure (3): Motor speed versus time.

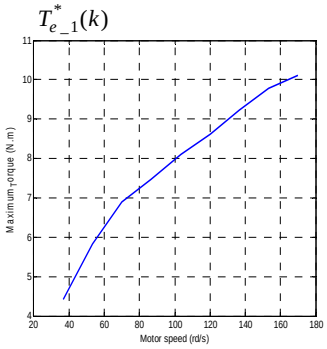

Figure (4): Maximum Torque versus motor speed.

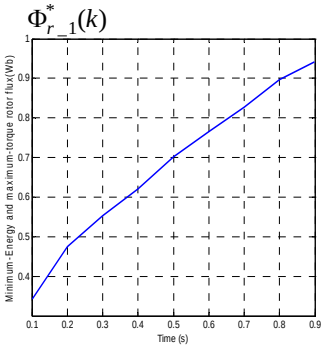

Figure (5): Optimal rotor flux versus motor speed.

7.2 Second area

The second area given by (50) occur when the motor is accelerated from 147rd/s to 290rd/s as shown in Figure (6). The maximum torque $T_{e\_2}^{*}(k)$ versus the motor speed is given in Figure (7) and the minimum-energy rotor flux trajectory: $\Phi_{r\_2}^{*}(k)$ is illustrated in the Figure (8).

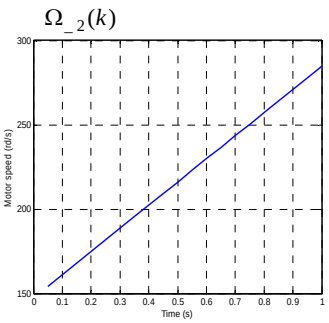

Figure (6): Motor speed versus time.

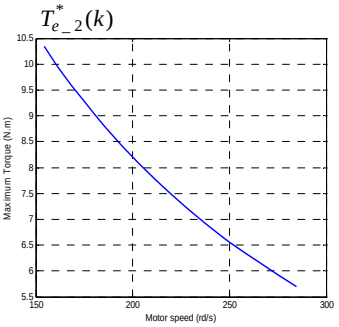

Figure (7): Maximum Torque versus motor speed.

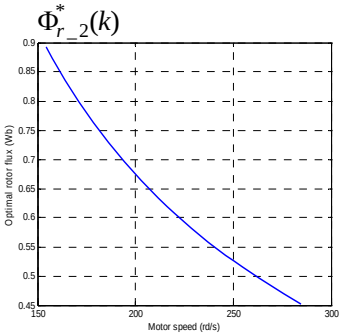

Figure (8): Optimal rotor flux versus motor speed.

7.3 Third area

the motor is accelerated from 335rd/s to 415rd/s as shown in Figure (9). This motor speed range characterize the start of the third area defined in (51). Figure (10) shows the evolution of the maximum torque $T_{e\_3}^{*}(k)$ versus the motor speed. The optimal rotor flux $\Phi_{r\_3}^{*}(k)$ is illustrated in Figure (11).

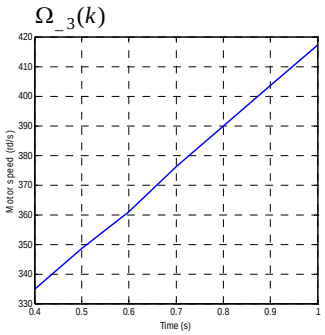

Figure (9): Motor speed versus time.

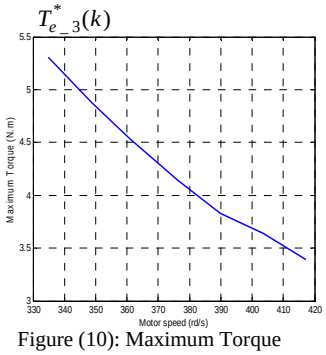

Figure (10): Maximum Torque versus motor speed.

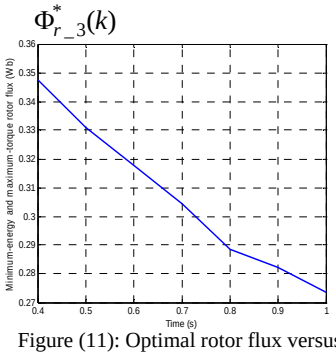

Figure (11): Optimal rotor flux versus motor speed.

In order to implement the optimal rotor flux reference over all the motor speed range, the three areas' optimal flux trajectories are compacted into one figure, given in Figure (12)

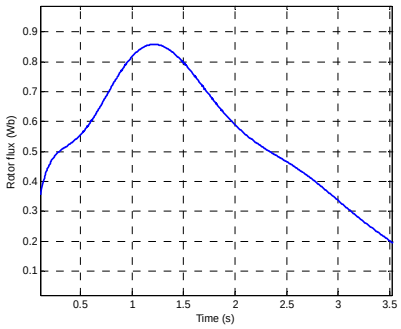

Figure (12): Optimal rotor flux versus motor speed.

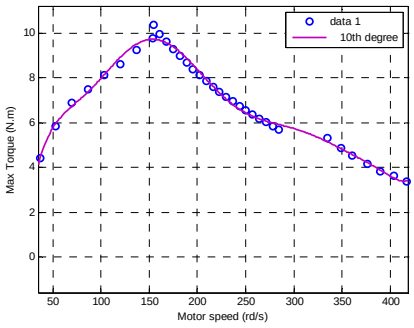

Figure (13): Maximum torque versus motor speed.

By the help of a least square method a 8th polynomial function degree can approximate the optimal rotor flux obtained by the areas' algorithms. This approximation is presented as follows:

$$\Phi_{r,ref}^{*}(t) = p_1 t^8 + p_2 t^7 + p_3 t^6 + p_4 t^5 + p_5 t^4 + p_6 t^3 + p_7 t^2 + p_8 t + p_9 \qquad (52)$$

where: p_1 = 0.0024159; p_2 = -0.055911; p_3 = 0.53407; p_4 = -2.7327; p_5 = 8.0706; p_6 = -13.678; p_7 = 12.173; p_8 = -4.5062 and p_9 = 1.0219.

The maximum torque obtained from the algorithms together is illustrated in Figure (13).

8. ORFOC strategy

By implementing the time-varying function of the optimal rotor flux reference in the RFOC, an accelerated motor speed mode is imposed to the control law: the motor speed varies with a ramp time-evolution from 30 rd/s (290 rpm) to 430 rd/s (4110 rpm). The load torque is assumed to be proportional to the speed. The torque closed-loop in the RFOC drive is initialized through applying a motor speed reference.
The rotor flux controller tracks the optimal rotor flux reference and brings out a direct stator current reference to the direct stator voltage controller. The quadratic stator current reference is limited to the stator currents boundary defined in (31). Both of the stator currents references are delivered to the rest of the ORFOC.
In the case of the second and the third areas, the quadratic stator voltage controller is limited by the boundary condition of the stator voltage given in (32).

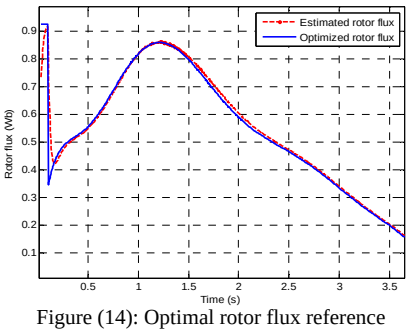

Figure (14): Optimal rotor flux reference and the estimated one.

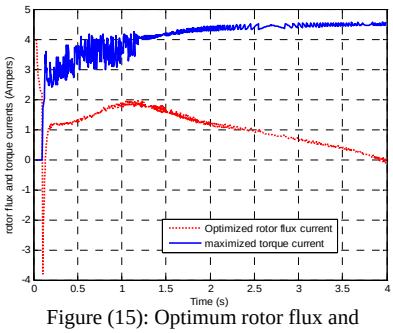

Figure (15): Optimum rotor flux and maximum torque currents

The tracked rotor flux and the optimal rotor flux is given in the Figure (14) and the Figure (15) illustrates the maximum torque and the rotor flux currents delivered to the stator voltage controllers in the ORFOC.

8. Simulation results

In order to bring out the effectiveness and the validity of the present ORFOC based on the Maximum Torque Control strategy (MTC), the obtained simulation results are compared to the RFOC used the standard approach of a Field Weakening Control (FWC). This approach is defined as follows:

$$\begin{aligned} \Phi_{ref}(t) = \Phi_{rated} &= MI_{sdn} && \Omega \le \Omega_{rated} \\ &= \Phi_{rated}\frac{\Omega_{rated}}{|\Omega|} && \Omega > \Omega_{rated} \end{aligned} \tag{53}$$

where Φ_{rated} =0.941 (Wb) for the induction motor under consideration and $\Omega_{rated} \cong 147.5 rd/s$

To provide a fair comparison of the two approaches, the maximum torque that can be delivered under the FWC has to satisfy the voltage and current constraints. In the other word, the direct stator currents I_{sd} is completely determined by (53) if the indirect stator current $|I_{sq}|$ is greater than $\sqrt{I_{s\max}^2 - I_{sd}^2}$ it takes this value, otherwise I_{sq} is left unchanged and it is at its optimum value.

Figure (16) illustrates the evolution of the maximum torque versus motor speed given by the ORFOC used the MTC strategy and the one given by the RFOC used the FWC strategy. It is interesting to note that the maximum torque based on the optimal flux reference is significantly better until the speed 3500 ($\approx 2.5\,\Omega_{rated}$). Above this value the standard field-weakening strategy becomes better.

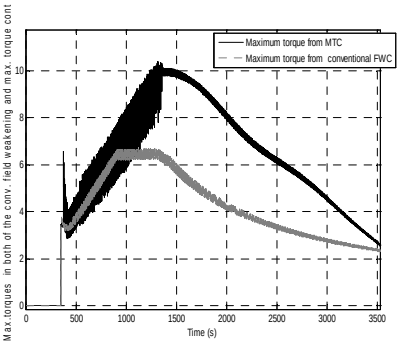

Figure (16): Maximum torque versus motor speed.

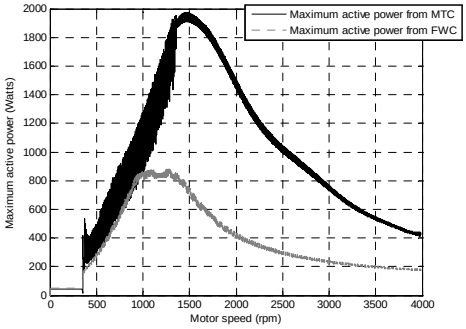

Figure (17): Maximum active powers versus motor speed.

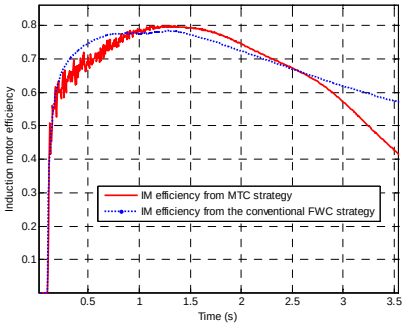

Figure (18): IM efficiencies.

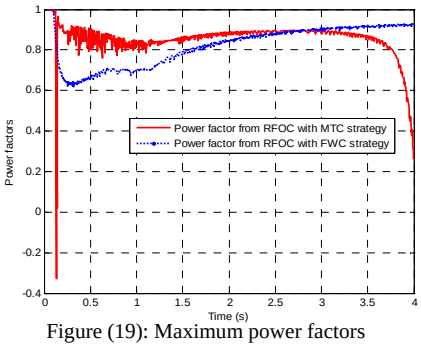

Figure (19): Maximum power factors versus motor speed.

As a consequence, the MTC strategy records also maximum active power better then the power obtained by the FWC strategy, as illustrates in the Figure (17). As defined by the optimal control problem in section 3, the maximum-torque rotor flux obtained by applying the Kuhn-tucker, results also by minimizing an energy-power cost function. Otherwise it gives also a maximum induction motor efficiency and power factor as illustrated respectively in Figures (18) and (19). Up to the fixed value $2.5\,\Omega_{rated}$, the standard approach register better efficiency and power factor level.

9. Conclusion

In this paper, an optimal control strategy was presented based on Kuhn-Tucker theorem and gives a maximum-torque rotor flux reference when the motor is accelerated. This approach entailed considering three cases in which the motor is at 1) the current limit, 2) both the current and voltage limits simultaneously, or 3) the voltage limit. As consequence, three algorithms are developed. By means of numerical resolution and for each step, several roots are obtained when solving equations from each algorithm. The boundary voltage and currents limits are used to find the appropriate roots. An interesting result was the significant increase in the torque available for accelerating the motor compared to the standard field-weakening approach when using the optimal rotor flux. For our laboratory induction motor used in this work, after $2.5\,\Omega_{rated}$, the standard approach register better results.

9. References

[1] J. Soltani, M. Hajian, G.R. Arab, "*Maximum Torque per Ampere Control of Induction Motor Drive without Mechanical Sensor*", International Conference on Control, Automation and Systems Oct. 14-17, **2008** in COEX, Seoul, Korea.

[2] Koichiro Nagata, Toshiaki Okuyama, Haruo Nemoto, and Toshio Katayama,"*A Simple Robuste Voltage Control of High Power Sensorless Induction Motor Drives With High Start Torque Demand*", IEEE Transaction On Industry Applications, Vol.44, NO.2, March/April **2008**.

[3] H. Abu-Rub, H. Schmirgel, and J. Holtz,"*Maximum Torque Production in Rotor Field Oriented Control of an Induction Motor at Field Weakening*", IEEE International Symposium on Industrial Electronics, ISIE, 4-7 June **2007**. Pages: 1159-1164

[4] Mario Cacciato, Alfio Consoli, Giuseppe Scarcella, and Giacomo Scelba, "*Indirect Maximum Torque per Ampere Control of Induction Motor Drives*", European Conference on Power Electronics and Applications, 2-5 Sept. **2007**. Pages: 1-10. .

[5] Domenico Casadei, Giovanni Serra, Angelo Tani, and Luca Zarri, "*A Robust Method for Field Weakening Operation of Induction Motor Drives with Maximum Torque Capability*",41 st IAS Annual Meeting. Conference Record of the 2006 IEEE Industry Application Conference, Vol. 1, 8-12 Oct. **2006**. Pages: 111-117. .

[6] S. Lim , and K. Nam, "Loss-minimising Control Scheme for Induction Motors", IEE, Proceeding-Electronic and Power Application, Vol. 151, No.4, July **2004**.

[7] Jul-Ki Seok, and Seung-Ki Sul, "Optimal Flux Selection of an Induction Machine in Flux-Weakening Region", IEEE Transaction On Power Electronics, Vol. 14, No. 4, July **1999**.

[8] Marc Bodson, John N. Chiasson, and Robert T. Novotnak,"A Systematic Approach to Selecting Flux References for Torque Maximization in Induction Motors", IEEE Transactions On Control Systems Technology, Vol. 3, No. 4, December **1995**.

[9] John Chiasson, *Modelling and High-Performance Control of Electric Machines*, IEEE Press Series on Power Engineering, John Willey & sons, Inc., Hobokon, New Jersey, **2005**.

[10] Radwan H. A. Hamid Amr M. A. Amin Refaat S. Ahmed Adel A. A. El-Gammal, "*New Technique for Maximum Efficiency and Minimum Operating Cost of Induction Motor based on Particle Swarm Optimization (PSO)*", Conference Student EEICT **2006**, the Soute University of electro technique and information technologies Czech republic.

[11] Hans.P Geering, *Optimal Control, with engineering application*, Springer-Verlog Berlin Heidelberg. **2007.**